Endocytosis targets exogenous material selectively to cathepsin S in live human dendritic cells, while cell-penetrating peptides mediate nonselective transport to cysteine cathepsins

Michael Reich,* Paul F. van Swieten,† Vinod Sommandas,* Marianne Kraus,* Rainer Fischer,‡ Ekkehard Weber,§ Hubert Kalbacher,|| Herman S. Overkleeft,† and Christoph Driessen*,[1]

*Department of Medicine II, ‡Institute for Cell Biology, and ||Medical and Natural Sciences Research Center, University of Tübingen, Tübingen, Germany; §Institute of Physiological Chemistry, University of Halle, Halle, Germany; †Leiden Institute of Chemistry, University of Leiden, Leiden, The Netherlands

Abstract: **The way the MHC II-associated proteolytic system of APC handles exogenous antigen is key to the stimulation of the T cell in infections and immunotherapy settings. Using a cell-impermeable, activity-based probe (ABP) for papain cathepsins, the most abundant type of endocytic proteases, we have simulated the encounter between exogenous antigen and endocytic proteases in live human monocyte-derived dendritic cells (MO-DC). Although cathepsin S (CatS), -B, -H, and -X were active in DC-derived endocytic fractions in vitro, the peptide-size tracer was routed selectively to active CatS after internalization by macropinocytosis. Blocking of the vacuolar adenosine triphosphatase abolished this CatS-selective targeting, and LPS-induced maturation of DC resulted in degradation of active CatS. Conjugation of the ABP to a protein facilitated the delivery to endocytic proteases and resulted in labeling of sizable amounts of CatB and CatX, although CatS still remained the major protease reached by this construct. Conjugation of the probe to a cell-penetrating peptide (CPP) routed the tracer to the entire panel of intracellular cathepsins, independently from endocytosis or LPS stimulation. Thus, different means of internalization result in differential targeting of active cathepsins in live MO-DC. CPP may serve as vehicles to target antigen more efficiently to protease-containing endocytic compartments. *J. Leukoc. Biol.* 81: 990–1001; 2007.**

Key Words: *antigen processing · lysosomal cysteine proteases · antigen-presenting cell · endocytic compartment · activity-base probe*

INTRODUCTION

Dendritic cells (DC) internalize exogenous antigen and deliver it to the MHC II-associated proteolytic machinery to generate antigenic peptides for the MHC II-mediated activation of T cells [1–3]. Human monocyte-derived DC (MO-DC) also provide attractive cellular tools for the manipulation of autoimmune disorders or the delivery of antigen-based cancer vaccines in vivo [4]. In such therapeutic vaccination protocols, MO-DC are usually exposed to soluble antigen or antigenic peptide, which is internalized by nonspecific means, processed by endocytic proteases, and loaded on MHC II so that ultimately, antigen-specific T cells are triggered. Understanding the rules that govern the transport of antigen to endocytic proteases and the successive processing pathway in MO-DC might help us to better exploit the therapeutic potential of these cells by maximizing the access of antigen to the MHC II-processing compartment or by facilitating the generation of the major immunogenic epitope in such therapeutic vaccines.

Soluble peptide or protein antigen is internalized by MO-DC in a nonselective manner via macropinocytosis and subsequently, reaches the endocytic compartment [1]. The majority of proteases in the endocytic compartment of DC belongs to the family of papain-like cysteine proteases [cathepsins (Cat) B, S, H, L, X], together with the aspartate proteases CatD and -E, as well as the asparagine-specific endopeptidase (AEP) [5–7]. This proteolytic system is not redundant in general, as genetic elimination of individual cathepsins resulted in defects in the processing and presentation of selected antigens as well as invariant chain (Ii) in vitro and in vivo [8–16]. As CatS is expressed selectively in professional APC and controls the rate-limiting step in Ii degradation, it is considered the key endocytic protease for antigen presentation in DC [5, 17]. The initial proteolytic attack on internalized antigen predetermines the subsequent processing pathway and can result in destruction or generation of immunodominant epitopes [18–20]. Thus, identification of this dominant "unlocking" protease(s) is crucial for the understanding of the processing pathway of a given antigen.

[1] Correspondence: Kantonspital St. Gallen, Dept. of Oncology and Hematology, Rorschachstr. 95, CH-9007 St. Gallen, Switzerland. E-mail: christoph.driessen@kssg.ch

Received October 2, 2006; revised December 1, 2006; accepted December 11, 2006.

doi: 10.1189/jlb.1006600

Fractionation studies revealed that lysosomes, late endosomes, and early endosomes differ with respect to the pattern of active proteases in all major types of APC [9, 21–23]. However, these types of studies required the disruption of major regulators of protease activity such as the endocytic pH gradient and the redox potential, so that they are of limited value for an analysis of the encounter between antigen and active proteases in intact cells. The use of chemical tools has overcome this limitation recently and allowed us to monitor the delivery of internalized material directly to endocytic proteases in viable APC [24]. Activity-based probes (ABP) bind specifically and irreversibly to the active center of papain-like cysteine proteases and enable the visualization of the targeted proteases via a detection tag [25]. ABP delivered to the endocytic compartment of live, murine bone marrow-derived APC via phagocytosis interacted progressively with different cathepsins, namely CatS, upon phagosome maturation in murine bone marrow (BM)-derived monocytes but not DC [24]. Human and murine APC and in particular, different types of DC vary significantly with respect to expression, activity, distribution, and regulation of endocytic proteases [6, 8–10, 21–23, 26, 27]. The pattern of endocytic proteases, which is encountered by antigen internalized by intact human MO-DC, is unknown.

Cell-penetrating peptides (CCP) serve as a carrier to cross the plasma membrane by direct permeation or endocytosis [28]. It has been suggested that CPP might also facilitate endocytosis, so that they could represent a strategy to increase the transport of exogenous material to protease-containing MHC II peptide-loading compartments in vaccination approaches. Indeed, the efficiency of a cancer vaccine in vivo was increased substantially by attaching antigenic material to CPP prior to vaccination [29]. However, neither the effect of CPP on the internalization of peptide-like antigen nor its influence on the pattern of proteases, which is targeted by such CPP-facilitated internalization, has been assessed directly in DC.

We here used ABP to address the delivery of exogenous material to active, papain-like cathepsins in human MO-DC. Internalization of ABP as soluble tracer, in conjugation with latex beads or protein, or facilitated by CPP modulated the patterns and efficiency of the delivery of exogenous material to endocytic proteases in intact, viable DC.

MATERIALS AND METHODS

Generation and characterization of DC

PBMC were isolated by Ficoll/Paque (PAA Laboratories, Austria) density gradient centrifugation of heparinized blood obtained from buffy coats. Isolated PBMC were plated (1×10^8 cells/8 ml flask) into tissue-culture flasks (Cellstar 75 cm^2, Greiner Bio-One GmbH, Germany) in RPMI 1640 (Gibco, Grand Island, NY, USA) supplemented with 10% FCS and antibiotics. After 1.5 h of incubation at 37°C, nonadherent cells were removed, and the adherent cells were cultured in complete medium supplemented with GM-CSF (Leukomax, Sandoz, Hanover, NJ, USA) and IL-4 (R&D Systems, Minneapolis, MN, USA) for 6 days [22]. This resulted in a cell population consisting of approximately 70% DC, as judged by flow cytometry. For induction of DC maturation, medium was supplemented with LPS (Sigma Chemical Co., St. Louis, MO, USA) at Day 6 for an additional 24 h. Murine BM-derived DC were prepared according to the protocol of Lutz et al. [30] from BM cells of BALB/c mice cultured in the presence of 200 U GM-CSF (produced by mouse myeloma strain P3X63)/ml for a total of 9 days. More than 90% of these cultures expressed CD11c, as assessed by flow cytometric analysis, and characteristic clustering of DC was observed by light microscopy. Human monocytes were enriched from buffy coats using a percoll gradient as described, resulting in 60–80% pure preparations of $CD14^+$ cells.

Flow cytometry analysis was performed using a FACSCalibur. Antibodies for immunophenotyping (Becton Dickinson, San Diego, CA, USA), OVA-FITC (Sigma Chemical Co.), and fluorochrome-coupled streptavidin latex beads (YG, Polysciences Inc., Warrington, PA, USA) were obtained commercially.

Affinity labeling of active cysteine proteases

General labeling procedure in cell lysates and endocytic fractions

JPM-565 and DCG-0N, a derivative of DCG-04 with identical labeling characteristics, were synthesized and purified as described previously [25, 31]. Crude endocytic extracts of at least 5×10^7 monocytes or human MO-DC were prepared according to the method described previously [23]. DC lysates were prepared from 5×10^5 immature DC in 2× lysis buffer [100 mM citrate/phosphate, 2 mM EDTA, 1% Nonidet P-40 (NP-40), pH 5] and were lysed for 30 min at 4°C, followed by removal of membrane fragments by centrifugation. Total endocytic protein (1.5 μg) of primary monocytes or 3 μg DC cell lysate protein was incubated with 10 μM DCG-0N, PS457, or DCG-0N preincubated in a ratio of 2:1 with streptavidin and 50 mM DTT at ambient temperature for 30 min. Reactions were terminated by addition of 6× SDS-reducing sample buffer and immediate boiling at 95°C for 10 min. Samples were resolved by 12.5% SDS-PAGE gel and then blotted on a polyvinylidene difluoride (PVDF) membrane (Amersham Biosciences, Piscataway, NJ, USA). After blocking with PBS-0.2% Tween 20 and 10% Roti®-Block (Roth, Karlsruhe, Germany) and extensive washing with PBS-0.2% Tween 20, the membrane was probed with Vectastain® (Vector Laboratories, Burlingame, CA, USA) in PBS-0.2% Tween 20 for 60 min, followed by washes with PBS-0.2% Tween 20. The ECL detection kit (Amersham Biosciences) was used for visualization.

For the flow cytometric-based analysis of the internalization of the respective constructs, YG-coupled strepatividin latex beads were purchased, which were otherwise identical to the particles used below (Polysciences Inc.), as well as FITC-coupled OVA (Sigma Chemical Co.). Con B was a kind gift from Hidde. Ploegh (Department of Pathology, Harvard Medical School, Boston, MA, USA). N-morpholinurea-homophenyl-leucyl-vinylsulfone (LHVS) was synthesized essentially as described [32]. E-64 and CA-074 were obtained from Sigma Chemical Co.

Labeling with DCG-0N coupled to streptavidin-coated latex beads

Crude endocytic fractions were prepared as described above. Streptavidin-coated, carboxylated latex beads (1 μm diameter, Polysciences Inc.) were incubated with different concentrations of DCG-0N for 1 h at room temperature. Beads were washed three times with PBS. The efficiency of the coupling and the washing steps were controlled by labeling cell lysates with beads pelleted after cenrifugation or with the supernatant after washing, respectively, as described above. To label cysteine proteases in live cells with DCG-0N coupled to streptavidin-coated latex beads, essentially, the procedure published for murine APC was used [24]. Streptavidin-coated, carboxylated latex beads were incubated with 100 μM DCG-0N for 1 h at room temperature. Beads were washed three times with PBS and resuspended in complete medium. Cells were plated on 24-well plates (1×10^7 cells/well) and pulsed for 1 h at 37°C with 300 μl medium containing DCG-0N-coated beads. After the pulse, excess beads were removed by centrifuging them four times at 2000 rpm for 2 min over a FCS cushion. Cells were washed with PBS and lysed with 100 μl 2× hot, reducing SDS sample buffer supplemented with 100 μM-free JPM-565. Lysates were boiled, and the DNA was sheared with a syringe and sonication. Samples were analyzed by 12.5% SDS-PAGE and streptavidin blotting.

Labeling of cysteine proteases in live cells with soluble DCG-0N and PS457

At least 1×10^6 DC per time-point were pulsed in complete culture medium (300 μl per time-point) for different times at 37°C with 25 μM DCG-0N or 10 μM PS457, if not mentioned otherwise. After the pulse, cells were washed to remove excess label at 4°C for four times in PBS. Where a chase was performed, cells were taken up in 37°C medium and then incubated for the

indicated additional times. After labeling, medium was removed, and cells were lysed with 50 μl 2× lysis buffer (100 mM citrate/phosphate, 2 mM EDTA, 1% NP-40, pH 7), supplemented with 100 μM-free JPM-565. SDS-reducing sample buffer (6×) was added to 50 μg total protein of each time-point and boiled immediately. Samples were resolved by 12.5% SDS-PAGE gel and then blotted on a PVDF membrane (Amersham Biosciences) and visualized as described above.

Labeling with ABP conjugated to streptavidin

Streptavidin (Jackson ImmunoResearch Laboratories, West Grove, PA, USA) was preincubated with DCG-0N or PS457 in PBS in a molar ratio of 1:2 for 1 h at room temperature and then added directly to the cells, which were pulsed, washed, and lysed as mentioned above. SDS-reducing sample buffer (6×), supplemented with 18 mM biotin (Serva, Germany), was added to 50 μg total protein of each time-point, followed by immediate boiling. Resolution by SDS-PAGE and detection were performed as described above.

Antisera, metabolic labeling, and immunoprecipitation

Rabbit antisera were generated against recombinant CatS and affinity-purified. Metabolic labeling and immunoprecipitation were performed exactly as described in refs. [9, 21, 33], using the Tu36 mAb, which recognizes human MHC II complexes in a conformational-specific manner. Equal numbers of human MO-DC were incubated in 500 μl methionine/cysteine-free medium supplemented with 10% FCS (Sigma Chemical Co.). Cells then were labeled by incubation with 500 μCi/ml [^{35}S]methionine-cysteine (Amersham Biosciences) at 37°C for 15 min. Medium was added in a 10–20× excess, and cells were chased at 37°C for different times. Cells were washed in PBS, frozen in liquid nitrogen, and stored at −80°C. After resolution by SDS-PAGE, the labeled polypeptides retrieved were visualized using a phosphorimager.

Synthesis of PS457

Where appropriate, removal of the 9-fluorenylmethyloxycarbonyl (Fmoc)-protecting group was accomplished by treatment of the resin-bound peptide with piperidine in N-methyl pyrrolidone (NMP; 1/4, v/v) for 20 min. Peptide-coupling steps were performed by treatment of the resin with a premixed (5 min) solution of the appropriate acid [5 equivalent (eq.)], 2-(6-chloro-1H-benzotriazole-1-yl)-1,1,3,3-tetramethylaminium hexafluorophosphate (5 eq.), and *N*,*N*-diisopropylethylamine (DiPEA; 6 eq.) in NMP for 1 h. Coupling efficiencies were monitored with the Kaiser test, and couplings were repeated if necessary. After coupling and deprotecting steps, the resin was washed with NMP (5′). Fmoc Rink amide resin (78 mg, 50 μmol) was elongated using automated, standard, Fmoc-based solid-phase peptide synthesis (SPPS) to give resin-bound [Arg(Pbf)]$_9$. The synthesis was continued by manual Fmoc-based SPPS to give protected and resin-bound PS457. The resin was washed extensively (alternating CH_2Cl_2-MeOH 3×; alternating CH_2Cl_2-Et_2O 3×). An aliquot of resin (100 mg, 16 μmol) was transferred into a clean vial, washed with CH_2Cl_2, and treated with trifluoroacetic acid (TFA)/H_2O/trisopropylsilane (0.7 ml, 95/2.5/2.5 v/v/v) for 2 h. The mixture was filtered into cold Et_2O, and the white precipitate was collected by centrifugation and decantation. The precipitate was washed (Et_2O), followed by HPLC purification of the crude product (linear gradient in Buffer B: 20–30% B in three-column volumes) to yield 4.3 mg (1.8 μmol, 11%) of product. ^{1}H nuclear magnetic resonance (NMR; D_2O, 295 K, DMX 600) included: δ, 7.08 (d, ^{2}H, J=7.9 Hz), 6.80 (d, ^{2}H, J=8.2 Hz), 4.58–4.55 (m, ^{1}H), 4.45–4.41 (m, ^{1}H), 4.38–4.35 (m, ^{1}H), 4.34–4.18 (m, ^{12}H), 4.13–4.09 (m, ^{1}H), 3.68 (br s, ^{1}H), 3.48–3.45 (m, ^{1}H), 3.30–3.25 (m, ^{1}H), 3.24–3.09 (m, ^{24}H), 3.03–2.86 (m, ^{4}H), 2.79 (s, ^{1}H), 2.69 (s, ^{1}H), 2.28–2.18 (m, ^{6}H), 1.80–1.20 (m, ^{61}H), 0.89–0.80 (m, ^{6}H); d, doublet; J, coupling constant; m, multiplet; s, singlet. Electrospray interface-mass spectrometry (ESI-MS): $C_{105}H_{189}N_{45}O_{24}S + {}^4H^+$ requires 625.5, found 625.4; $C_{105}H_{189}N_{45}O_{24}S + {}^3H^+$ requires 833.7, found 833.6.

Solvents used in the SPPS, DiPEA and TFA, were all of peptide-synthesis grade (Biosolve) and used as received. The protected amino acids, Rink amide p-methylbenzhydrylamine resin (0.78 mmol g–1) was obtained from NovaBiochem (Switzerland). Ethyl (2S,3S)oxirane-2,3-dicarboxylate was prepared as described. Fmoc-Lys(Mtt)-OH was from Senn Chemicals (Switzerland); SPPS was carried out using a 180°C variable rate flask shaker (St. John Associates, Inc., Beltsville, MD, USA) or on a 443A peptide synthesizer (Applied Biosystems, Foster City, CA, USA). Liquid chromatography/MS analysis was performed on a Jasco HPLC system (detection simultaneously at 214 and 254 nm) coupled to a Perkin Elmer Sciex API 165 MS equipped with a custom-made ESI. An analytical Alltima C18 column (Alltech, Ireland; 4.6 mmD, 250 mmL, 5 μm particle size) was used; buffers: A = H_2O; B = CH_3CN; C = 0.5% aq TFA. For reversed-phase HPLC purification of two and four, a Biocad "Vision" automated HPLC system (PerSeptive Biosystems, Inc., Framingham, MA, USA) was used. The applied buffers were A, B, and C. ^{1}H-NMR spectra were recorded with a Bruker DMX 600 instrument at 600 MHz with chemical shifts (δ) relative to tetramethylsilane.

Quantification by densitometry

NIH ImageJ was used for quantification of the intensity of labeling for the active polypeptides visualized by affinity labeling (http://rsb.info.nih.gov/ij/).

RESULTS

Here, we applied a strategy to human DC, which allows visualization of the rendezvous between individual, endocytic, cyteine proteases and internalized, exogenous material taken up by live APC via different modes of transport. An ABP for cysteine proteases is internalized via endocytosis or a CPP as a shuttle, reaches endocytic compartments, and interacts with the local proteolytic contents by covalent binding to the catalytic center of active cysteine proteases. As an ABP, we used DCG-0N, a derivative of the peptide epoxides JPM-565 and E-64, which targets papain-like cysteine proteases specifically. The labeling characteristics of DCG-0N are identical to its mother compounds DCG-04 and to JPM565 (**Fig. 1A**) [24]. Proteases reached by the probe after internalization are irreversibly bound and can be visualized after cell lysis and SDS electrophoresis by streptavidin blotting against the biotin moiety of the probe so that different signal intensities of a particular protease polypeptide correspond directly to different amounts of the active protease species reached by the tracer in the living cell.

Different patterns of active, papain-like cysteine proteases are visualized by the active, site-directed probe DCG-0N in primary human monocytes and MO-DC

The affinities of DCG-0N for the different papain-like cysteine proteases are in a similar order of magnitude, but not identical, and also, the total amounts of a given active protease vary between different types of APC. To account for differences in protease labeling, which might result solely from different affinities of the probe for various cathepsins, differences in the total amounts of an individual protease or subsaturating amounts of the probe, rather than from differential delivery of the probe to active cathepsins in intact APC, we performed titration experiments with crude endocytic fractions incubated with increasing concentrations of DCG-0N in vitro, followed by a streptavidin blot. The detected polypeptides in the 20- to 40-kD range were identified via immunoprecipitation with antibodies directed against individual cathepsins as well as by MS-based sequencing after pull-down with streptavidin beads [21], allowing the identification of CatB, CatH, CatL, CatS, and CatX (Fig. 1B). In endocytic fractions derived from primary monocytes, CatS was detected at the lowest concentration of label, followed by CatB, CatH, and CatX, with increasing

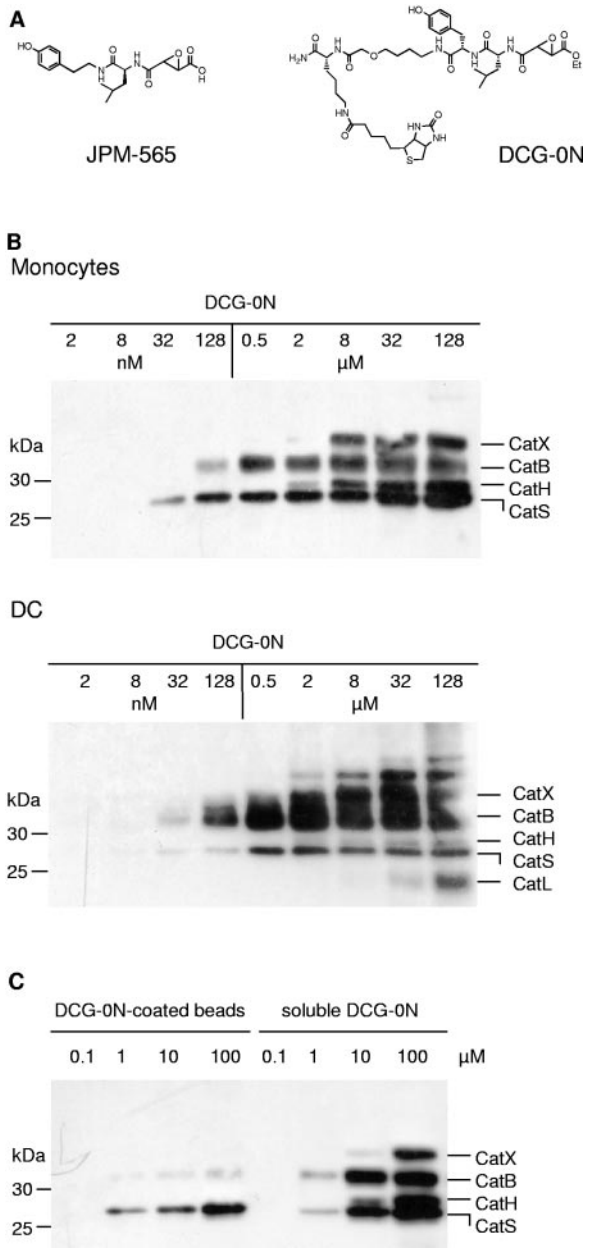

Fig. 1. Papain-like, cysteine proteases recognized by the active, site-directed probe DCG-0N in endocytic fractions of primary monocytes and MO-DC. (A) Structure of the active, site-directed probe JPM-565 and its biotinylated analog DCG-0N. (B) Titration of DCG-0N for the labeling of endocytic fractions of human monocytes (upper panel) and human MO-DC (lower panel) at pH 5. Lysates were incubated with increasing concentrations of DCG-0N. Proteins were separated by SDS-PAGE on a 12.5% gel, and reactive polypeptides were visualized by streptavidin blotting ($n=3$). (C) Effect of the immobilization of DCG-0N by conjugation to streptavidin-coated latex beads on the selectivity of labeling. Endocytic extracts of monocytes were incubated for 30 min at room temperature with latex beads preincubated with different concentrations of DCG-0N or with the soluble tracer alone at the same concentrations prior to visualization of the labeled species ($n=5$).

amounts of DCG-0N. In endocytic fractions of human MO-DC, CatB was the protease that could be visualized at the lowest concentration of DCG-0N, and CatS was only detected with higher amounts of DCG-0N. CatX and CatL were only visualized at increasing concentrations of DCG-0N. Thus, different relative amounts of individual cathepsins in a given cell type (DC vs. monocytes) also account for differential labeling patterns of proteases, especially at low concentrations of label. Of note, in human DC, active CatS appeared to be less prominent, compared with the remaining cysteine cathepsins, than in human monocytes, especially under the limiting conditions of subsaturating amounts of label. These individual labeling patterns in crude endocytic fractions served as the basis to account for the specific delivery of label to a given protease after internalization by intact cells, as analyzed in the following experiments.

DCG-04 coupled to streptavidin-coated latex beads has served as a tool to assess the delivery of exogenous material taken up by phagocytosis to endocytic proteases in murine BM-derived APC [24]. To control for the possibility that binding of DCG-0N to latex beads could affect the reactivity or selectivity of the probe, endocytic extracts from primary human monocytes were incubated with the soluble probe or with DCG-0N coupled to streptavidin-latex beads. Labeled protease species were then visualized by SDS-PAGE and antibiotin blot (Fig. 1C). The immobilization of DCG-0N on streptavidin beads favored labeling of CatS over the other cathepsins so that CatB was labeled poorly, and CatX and CatH could not be visualized at all. Thus, the immobilization of DCG-0N on latex beads affects the selectivity of labeling, which might induce artifacts when a proteolytic environment is sampled using DCG-0N immobilized on beads.

Human MO-DC poorly internalize latex beads via phagocytosis

When murine BM-derived DC were incubated with fluorochrome-labeled latex beads, they internalized these beads efficiently by phagocytosis at 37°C, but not at 4°C, as assessed by flow cytometry, consistent with the published data [24] (**Fig. 2**). By contrast, human MO-DC only poorly ingested the same type of beads in vitro under otherwise identical conditions, highlighting the biological differences between both types of DC preparations. However, human MO-DC efficiently internalized soluble, fluorochrome-labeled OVA by endocytosis (1.4%-positive cells at 4°C compared with 83.12% at 37°C). As soluble antigen internalized by endocytosis represents one of the most common modes of antigen delivery to MO-DC in vitro in immunotherapy settings, immobilization of the ABP influences its labeling characteristics, and human MO-DC only poorly internalize exogenous material by phagocytosis in vitro, we analyzed the encounter of exogenous material internalized by MO-DC via endocytosis, not phagocytosis, in the following experiments.

Delivery of exogenous DCG-0N to active papain-like cathepsins by endocytosis in human DC

To monitor the delivery of internalized material to the protease pool of MO-DC, intact DC were incubated for 1 h at 37°C with 5 μM-soluble DCG-0N. As controls, we included DC incubated under the same conditions with streptavidin-coated latex beads previously coupled with DCG-0N, as well as the same amount of cells pulsed with soluble DCG-0N at 4°C. Excess beads were removed by extensive washing, and cells were lysed at pH 7 in 2× lysis buffer containing excess, nonbio-

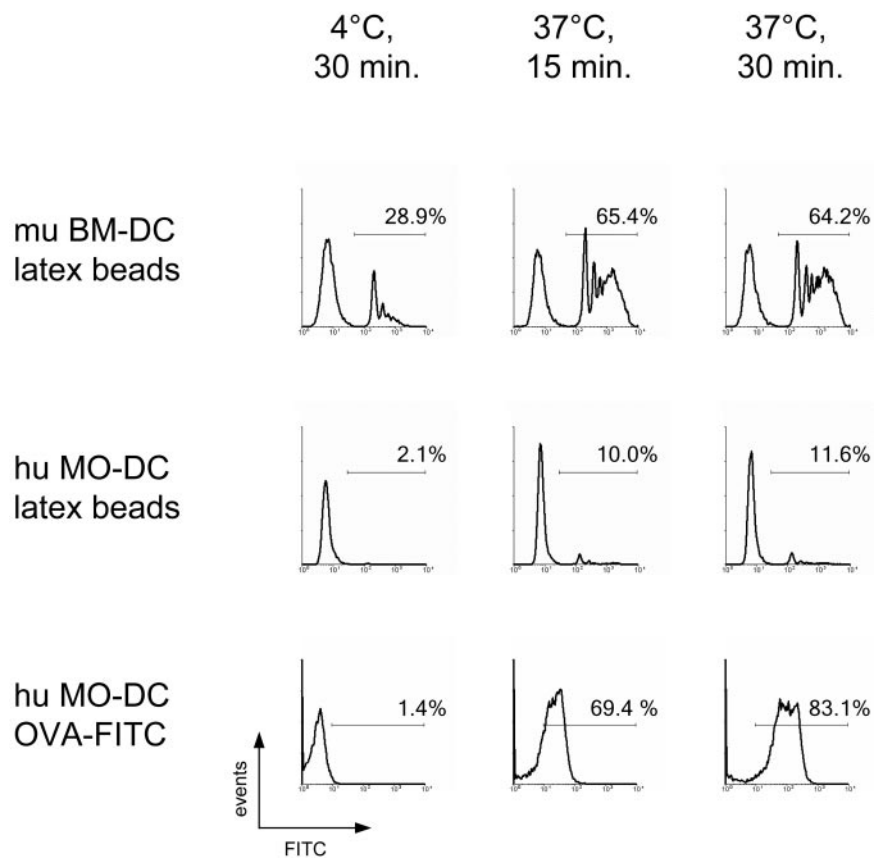

Fig. 2. Different efficiency of phagocytosis-mediated internalization between human MO-DC and murine BM-derived DC. Murine (mu) BM-derived DC or human (hu) MO-DC were incubated with FITC-labeled latex beads for up to 30 min at 4°C and at 37°C, respectively. Similarly, human MO-DC were incubated in the presence of OVA FITC. After washing the cells at the appropriate time-points, cellular fluorescence was analyzed by flow cytometry (n=3).

tinylated JPM-565 to largely exclude that proteases liberated upon cell lysis could bind to the probe postlysis. For direct comparison of the fraction of active proteases labeled after internalization of the probe by MO-DC in vivo with the total protease pool present in these cells, a total cell lysate was prepared from a portion of the same DC sample, lysed at pH 5, and labeled with DCG-0N after cell lysis. All samples were boiled at 95°C in 6× reducing SDS sample buffer, resolved by electrophoresis, and analyzed by streptavidin blotting to visualize the DCG-0N-modified polypeptides (**Fig. 3A**).

In contrast to murine BM-derived DC [24], live human MO-DC did not result in labeling of active cathepsins after coincubation with DCG-0N-coated latex beads at 37°C (Fig. 3A, Lane 3), consistent with the poor uptake of latex beads by MO-DC, as judged by flow cytometry. Soluble DCG-0N, however, decorated active cathepsins when intact human MO-DC were exposed at 37°C (Fig. 3A, Lane 4), in contrast to the 4°C control (Fig. 3A, Lane 5). Although in crude endocytic DC fractions, active CatB was labeled much stronger by the probe than CatS (Fig. 3A, Lane 1), internalization of the probe by live human DC clearly favored labeling of CatS with little targeting of CatB and without significant visualization of CatX after endocytosis-mediated delivery (Fig. 3A, Lane 4). Thus, soluble DCG-0N, internalized by macropinocytosis, is routed selectively to a compartment enriched with CatS activity in human MO-DC.

To resolve the rendezvous between individual cysteine proteases and exogenous matter internalized by pinocytosis as a function of time, DC were incubated with soluble DCG-0N for up to 120 min. We observed a rather selective, time-dependent increase in labeling of active CatS between 0 and 30 min, visible already after 9 min of uptake, consistent with an early endosomal localization of active CatS (Fig. 3B, left). Longer incubation, up to 120 min, did not result in further changes in the labeling results (data not shown). The labeling intensities for CatB and CatX were low and almost stable over time, indicating a negligible exposure of exogenous peptide-size matter delivered by pinocytosis to these cathepsins in live human DC. Again, incubation of cells with soluble DCG-0N at 4°C for the same time did not result in significant visualization of protease polypeptides, confirming the active uptake of DCG-0N by live DC, as opposed to postlysis artifacts or nonspecific, passive transition of the plasma membrane by DCG-0N. When DC were cultured for 24 h with LPS and then pulsed with DCG-0N, the time-dependent increase in labeling of active CatS was abolished (Fig. 3B, right), consistent with the low rate of endocytosis of activated DC, as confirmed by flow cytometry analysis (not shown).

In contrast to monocytes, resting DC are capable of preserving intact antigen within endocytic compartments for several hours before antigen breakdown is initiated by DC activation, a feature that has been suggested to contribute to the ability of DC to provide antigenic memory. It was tempting to speculate that the CatS-restricted delivery of antigen to endocytic proteases observed in DC might represent the molecular basis for the low rate of antigen processing in resting DC. We therefore assessed the delivery of soluble DCG-0N to endocytic proteases in primary human monocytes enriched by Percoll gradient centrifugation in an identical manner (Fig. 3C). Similar to MO-DC, CatS was reached preferentially by the internalized

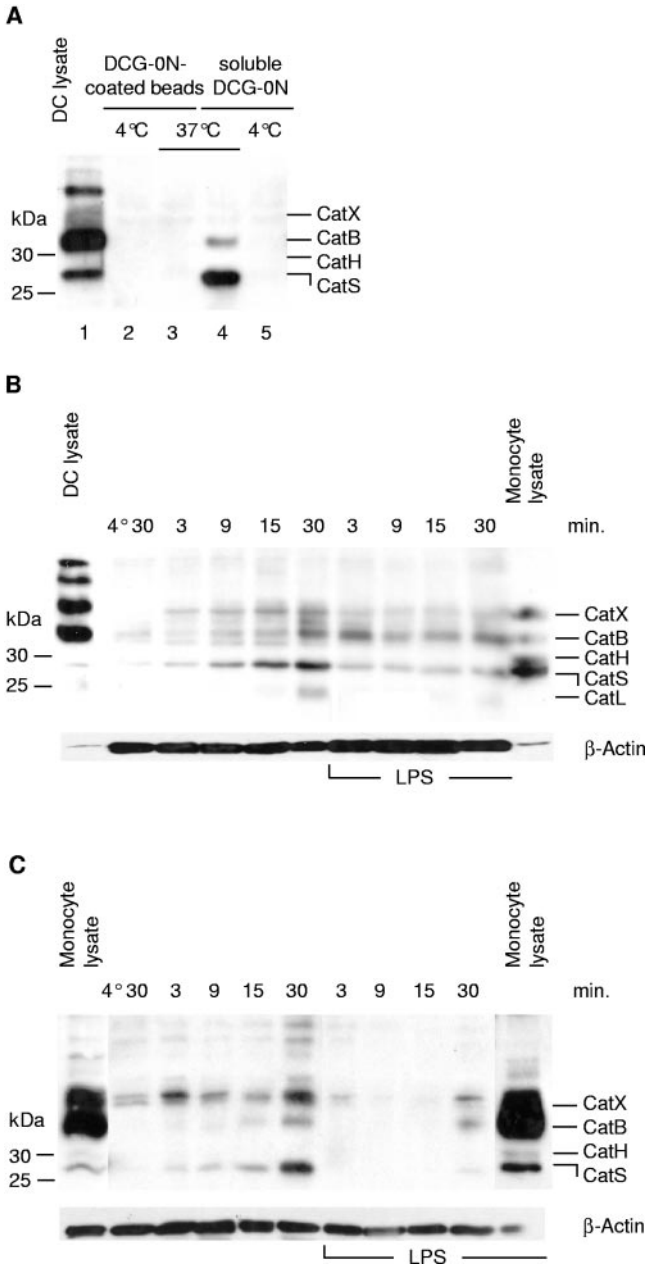

Fig. 3. Delivery of DCG-0N to cathepsin-containing compartments. (A) Live DC were incubated for 1 h at 37°C with 25 μM-soluble DCG-0N or streptavidin-coated latex beads preincubated with DCG-0N at the same concentration. After extensive washing, cells were lysed at pH 7 in lysis buffer containing 100 μM JPM-565 and boiled in 6× concentrated, reducing sample buffer. Incubation for 1 h at 4°C served as control for the active internalization of the protease label. Lysates from DC labeled with DCG-0N served as standards to identify the labeled protease species and to relate their signal intensity to their relative abundance in the cell (n=6). (B) Intact DC were incubated with soluble DCG-0N at 37°C for different periods of time, as indicated, with or without prior exposure to LPS for 24 h. Incubation with DCG-0N for 30 min at 4°C served as control for the active internalization of the protease label. After extensive washing, cells were lysed in 2× lysis buffer containing 100 μM JPM-565, and labeled protease species were visualized by SDS-PAGE/antibiotin blot. DC and monocyte-derived cell lysates served as controls as above (n=5), and comparable total protein load was confirmed by Western blot against β-actin. (C) Intact, primary monocytes enriched by percoll gradient centrifugation were incubated with soluble DCG-0N at 37°C for different periods of time, as indicated, with or without prior exposure to LPS for 24 h as detailed above (n=6). Active endocytic proteases reached by the tracer were visualized as in B. Western blot analysis for β-actin served as a loading control.

tracer in monocytes, and CatB and CatX were decorated relatively poorly and in variable amounts in individual experiments, most likely representing postlysis artifacts. Similar to the results observed with DC, a consistent and reproducible increase in labeling intensity was only observed for CatS, but not for CatB or CatX. Prior stimulation of monocytes by LPS markedly reduced the delivery of exogenous DCG-0N to endocytic proteases, also paralleling the results obtained with MO-DC. Thus, the preferential targeting of exogenous material to active CatS is not a unique feature of DC but can likewise be observed in monocytes and is therefore unlikely to represent the basis for antigen memory observed in DC.

Activity of the vacuolar adenosine triphosphatase (ATPase) modulates the recruitment and stability of CatS targeted by internalized material

To dissect the intracellular delivery of cathepsins to the internalized ABP, intact DC were incubated with soluble DCG-0N at 37°C for 10 min (pulse), followed by extensive washing to remove a noninternalized label and a chase at 37°C for 0–30 min, respectively, at 37°C. Control cells were incubated at 4°C for the pulse (4°C, 0) or for the pulse and the chase period (4°C, 30), respectively. Labeled protease species were visualized by SDS-PAGE/antibiotin blot (**Fig. 4A**). In untreated cells, the CatS signal increased selectively during the 0- to 30-min chase period (compare with 4°C, 30 min control). Extending the chase to 120 min yielded comparable results and did not result in increased labeling of additional protease polypeptides (data not shown). This indicated that active CatS, but not CatB, CatH, or CatX, was preferentially routed toward or activated within DCG-0N-containing endosomes within 30 min after internalization by intact human MO-DC. CatS is therefore the most likely candidate for the initial proteolytic attack on newly internalized, peptide-type antigens in human MO-DC.

The endocytic machinery of DC is regulated largely by the activity of the vacuolar H^+-ATPase: Although low activity characterizes resting DC with high endocytic activity, DC maturation by stimuli such as LPS results in ATPase activation and a drop in vacuolar pH. Addition of Con B, an inhibitor of the H^+-ATPase, blocks orderly transport, especially at the early-to-late endosomal transition [34]. To further characterize the mechanism of the recruitment of active CatS to the internalized ABP, we added Con B to one-half of the sample prior to the pulse (Fig. 4A, upper right). Con B blocked labeling of active CatS when DCG-0N was internalized by live cells but did not affect the visualization of active CatS when total cell lysates of MO-DC were treated with the same amount of the drug for 60 min directly prior to lysis. This indicated that Con B disrupted the intracellular delivery of internalized DCG-0N to active CatS rather than interfering with cellular CatS activity. Thus, the vacuolar H^+-ATPase is required for the selective delivery of exogenous material to active CatS in intact human MO-DC.

LPS-induced DC maturation leads to increased activity of the endocytic ATPase. When the intracellular delivery of DCG-0N to active cathepsins was analyzed in the same type of pulse-chase experiment as above with DC stimulated with LPS, active CatS was visualized with inverse kinetics during the

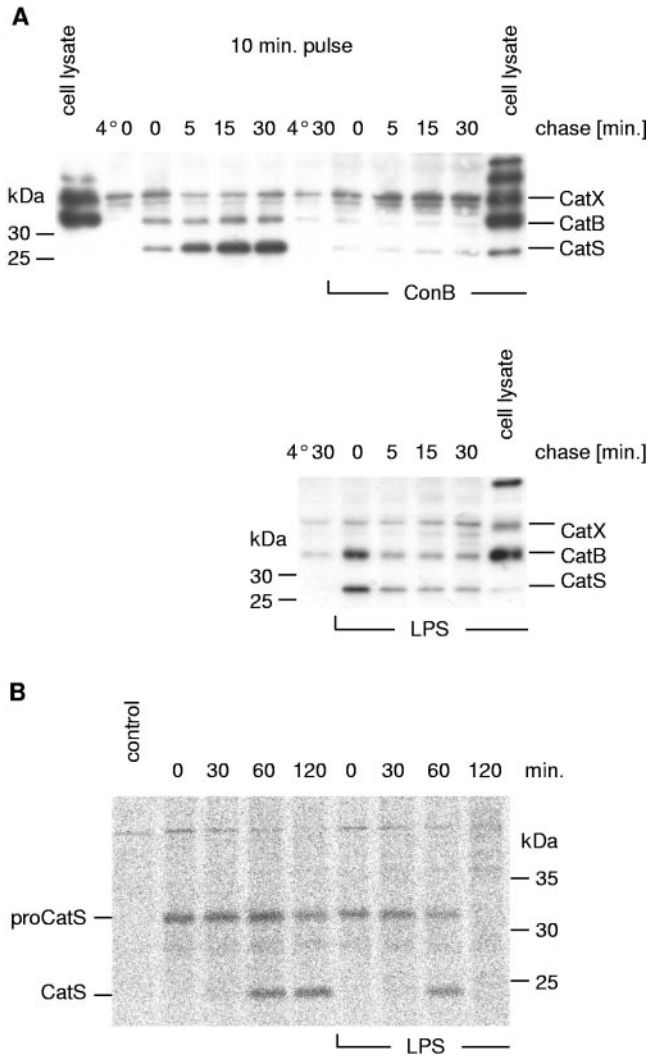

Fig. 4. (A) DC were left untreated (upper left) or pretreated with 20 nM Con B for 60 min (upper right) or with LPS for 24 h (lower right). Cells were pulsed with soluble DCG-0N at 37°C for 10 min. Following extensive washing, cells were chased at 37°C for the times indicated (chase). After each time-point, cells were lysed, proteins were separated by SDS-PAGE on a 12.5% gel, and reactive proteases were visualized by streptavidin blotting as above ($n=4$). (B) Analysis of the biosynthesis, maturation, and degradation of CatS in DC. Cells left unstimulated or stimulated with LPS for 24 h were pulse-labeled with ^{35}S Met/Cys for 15 min, followed by a chase for up to 2 h. After lysis, CatS was retrieved by immunoprecipitation using a CatS antiserum. After exposure to 95°C in 6× concentrated, reducing sample buffer, polypeptides retrieved were separated by SDS-PAGE, followed by autoradiography using a phosphorimager. One representative result from three independent experiments is shown ($n=3$).

chase (4A, lower right): Labeling intensity for CatS decreased continuously over the 30-min chase. Because of the irreversible nature of binding of the probe to active CatS, this suggested degradation of the bound probe, the labeled protease, or both.

To differentiate between these two possibilities, we assessed the biosynthesis, maturation, and stability of CatS in resting and LPS-stimulated DC by metabolic labeling and immunoprecipitation of CatS. DC were pulse-labeled with ^{35}S Met/Cys for 15 min at 37°C, followed by different chase periods in the presence of excess, nonradioactive Met/Cys. At each chase-point, cells were washed and lysed, and CatS was retrieved by immunoprecipitation using a specific antiserum. The bound material was eluted in 95°C-reducing SDS sample buffer, followed by resolution of the retrieved polypeptides by SDS-PAGE and autoradiography (Fig. 4B). In resting DC, proCatS migrating at 32 kD was visualized exclusively after the pulse. After 30 and 60 min of chase, constant amounts of proCatS were detected. Mature CatS emerged at the 60-min chase-point, and proCatS was still present in comparable amounts, suggesting that at this time-point, proCatS was still being synthesized, and mature CatS was converted from its zymogen. After 120 min of chase, mature CatS remained stable, and the amounts of the labeled proform decreased. Thus, proCatS reaches the endocytic compartment roughly 60 min after biosynthesis in resting human DC and is stable and progressively activated from its zymogen for at least another 60 min. LPS-stimulated DC were analyzed the same way: Mature CatS also emerged after 60 min of chase, suggesting that DC maturation did not grossly influence the conversion from proCatS to active CatS. However, already at the 60-min chase-point, the amount of proCatS was reduced compared with the 30-min chase-point or the nonstimulated sample, and mature CatS was also present, only in lower amounts than in the nonstimulated sample. At the 120-min chase-point, radiolabeled CatS and proCatS were consistently absent from LPS-stimulated DC, in stark contrast to nonstimulated DC, demonstrating degradation of CatS 1–2 h after biosynthesis in LPS-stimulated DC. Complete degradation of active, newly synthesized CatS in LPS-activated human DC can therefore be observed within 60 min after entering the endocytic compartment, in contrast to resting DC, and therefore, DC maturation controls the levels of mature CatS in an activation-dependent manner via endocytic degradation of the protease.

Conjugation of DCG-0N to streptavidin increases CatS-targeted delivery

Soluble peptides and whole-size proteins are being used to deliver antigen to MO-DC in vitro for immunotherapy. Whole-size sugars or proteins such as Dextran or HRP, at least in part, use endocytosis mediated by mannose receptor-binding, which might facilitate endocytosis and hence, delivery to endocytic proteases [35, 36]. Thus, to increase the delivery of exogenous material to active cathepsins, we generated a larger protein-like tracer by conjugating DCG-0N to streptavidin prior to exposure to live DC, which were pulsed at 37°C for 10 min using soluble 5 μM DCG-0N or the same amount of the probe prebound to 2.5 μM streptavidin prior to the pulse. After removal of noninternalized label by washing, cells were chased for up to 30 min, and labeled protease species were visualized by a SDS-PAGE/antibiotin blot (**Fig. 5**). Conjugation of DCG-0N to streptavidin significantly improved delivery of the probe to active cathepsins in intact DC, compared with soluble DCG-0N. Labeling efficiency of CatS increased nearly fivefold with streptavidin-bound DCG-0N (lower panel), compared with delivery by the nonconjugated tracer. It is important that the preferential labeling of active CatS was also preserved when the uptake of the tracer was facilitated by prior conjugation to a protein: Labeling of CatS remained clearly dominant over labeling of active CatX and CatB in intact DC, in contrast to

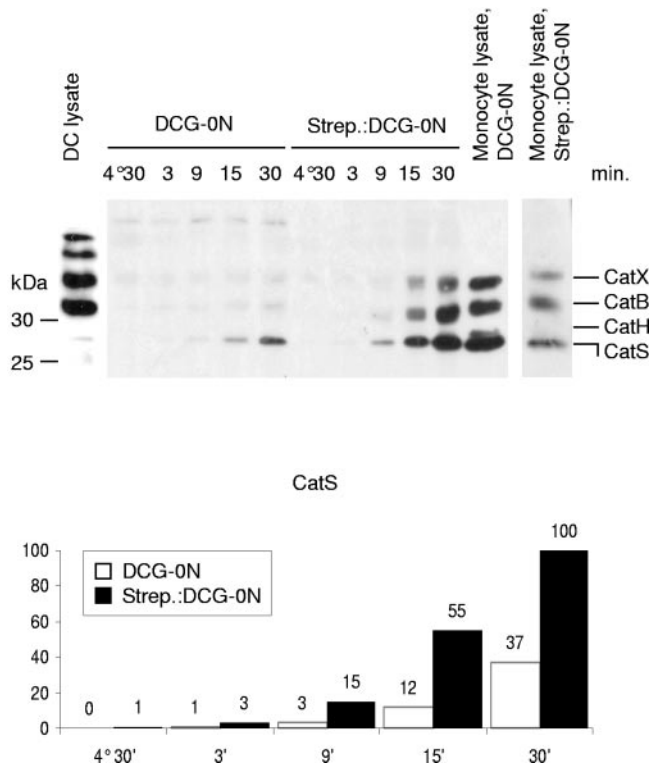

Fig. 5. Conjugation of DCG-0N to streptavidin increases the efficiency of protease delivery. (Upper panel) DC were pulsed with soluble DCG-0N or with DCG-0N (5 μM each), preincubated with streptavidin at a 2:1 molar ratio at 37°C for different periods of time. After extensive washing, cells were lysed in 2× lysis buffer containing 100 μM JPM-565, and the targeted, active polypeptides were visualized as above (n=2). Labeling of DC and monocyte lysates with soluble DCG-0N as well as with streptavidin-prebound DCG-0N (1 μM) served as controls. (Lower panel) Densitometric quantification of the relative amounts of active CatS targeted by soluble or streptavidin-bound DCG-0N in live human DC, as deduced from the upper panel.

the labeling pattern observed in the total DC lysate. As expected, active cathepsins were not decorated using soluble DCG-0N or the DCG-0N-streptavidin construct for 30 min at 4°C. Thus, protein-size cargo is transported to active cathepsins more efficiently than the peptide-size, soluble tracer in live human MO-DC. It is important that both types of delivery result in preferential targeting of exogenous material to active CatS.

A CPP increases delivery to cathepsin-containing compartments

CPP can increase the efficiency of peptide vaccines in vivo, possibly by facilitating the transport of the peptide vaccine into endocytic compartments of APC. To directly assess the effect of the conjugation of a peptide to a CPP on its delivery to endocytic proteases in DC, we synthesized a DCG-0N-derivative conjugated to a nonarginine CPP (PS457, **Fig. 6A**). Monocyte-derived endocytic fractions were incubated consecutively with PS457 for the visualization of the labeled polypeptides. Although no protease polypeptides were visualized by PS457 in the 95°C-preheated and the 25-μM E-64-treated samples (Fig. 6B, Lanes 1 and 2), two polypeptides were weakly visualized in the sample labeled with PS457 (Fig. 6B, Lane 3). The signals migrated slightly higher than the respective signals for CatS and CatB in the DCG-0N-labeled sample (Fig. 6B, Lane 6), consistent with the molecular weight of the PS457 probe. Note that the intensity of labeling with DCG-0N (Fig. 6B, Lane 6) is substantially higher compared with labeling with PS457 at equimolar concentrations in crude endocytic fractions (Fig. 6B, Lane 3). Addition of the CatS inhibitor LHVS (25 nM) and the CatB inhibitor CA-074 (1 μM) eliminated labeling of active CatS and reduced labeling of active CatB (Fig. 6B, Lane 4) and eliminated active CatB labeling (Fig. 6B, Lane 5), respectively, consistent with the identity of these polypeptide species as CatS and CatB in PS457-labeled cell lysates.

To test protease delivery of PS457 in intact DC, we pulsed DC with 10 μM soluble DCG-0N or PS457 for 1 h at 37°C with 4°C controls and labeling of cell lysates, respectively, as before (Fig. 6C). As expected, soluble DCG-0N preferentially decorated active CatS at 37°C but did not label cathepsins at 4°C in live DC (Fig. 6C, Lanes 2 and 3). By contrast, PS457 visualized the entire set of active cathepsins already at 4°C (Fig. 6C, Lane 5), demonstrating that it reaches cathepsin-containing compartments efficiently, independent from endocytosis activity. In fact, PS457 labeled active cathepsins in intact DC at 4°C with efficiency comparable with DCG-0N at 37°C. Given the poor labeling characteristics of PS457 compared with DCG-0N in cell lysates, passive transition of the plasma membrane facilitated by the nonarginine CPP is at least in the same order of magnitude as the rate of fluid-phase endocytosis of MO-DC, which is known to be particularly high. Thus, CPP represent a powerful tool to deliver peptide-sized material to endocytic compartments, independently from active endocytic transport. Uptake of PS457 at 37°C significantly increased the amounts of proteases targeted by the probe, and LPS-induced down-modulation of endocytic internalization down-regulated this delivery. PS457 is thus internalized by a combination of endocytosis and passive, transport-independent transition of the cell membranes. In stark contrast to endocytosis-mediated uptake of DCG-0N, however, passive internalization of PS457 did not target CatS-containing compartments selectively but resulted in equally efficient delivery of the probe to active CatB and CatX.

When intact DC were exposed to both compounds (DCG-0N vs. PS457) in a pulse-chase format (Fig. 6D), these differences became even more obvious: Although at low concentrations of label (10 μM), the signal derived from exposure of the cells to DCG-0N remained at or below the threshold of detection, robust labeling of active cathepsins could be observed after incubation of DC with 10 μM PS457, where maximum signal intensity was reached already after 15 min of chase. Note that CatB was visualized much stronger than CatS, similar to the pattern in the DC lysate and in contrast to the pattern observed after internalization of DCG-0N (compare also Fig. 3B). We conclude that the delivery of exogenous, peptide-like material to active endocytic proteases is increased significantly when this material is conjugated to the polycationic shuttle device. Under these conditions, exogenous material can enter endocytic compartments of DC independently from active transport and is routed to endocytic proteases in a nonselective manner in contrast to endocytosis-mediated delivery.

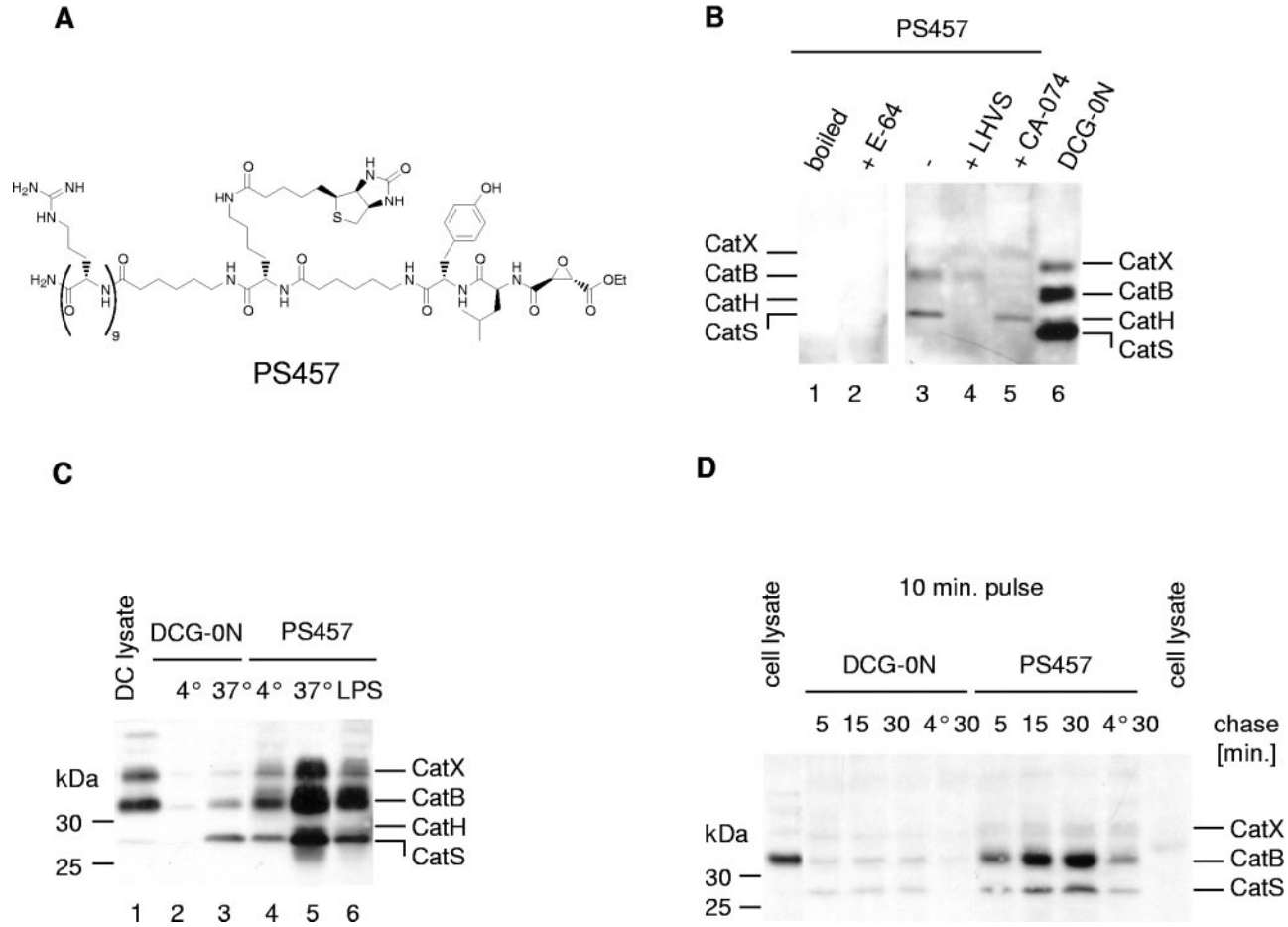

Fig. 6. CPP increase delivery to protease-containing compartments in DC. (A) Structure of the CPP analog PS457, consisting of a DCG-0N core attached to a nonarginine cell-penetrating, transport device. (B) Labeling of active cysteine proteases by PS457. Cytosolic extracts of human monocytes were incubated with 10 μM DCG-0N or PS457, respectively, for 30 min at room temperature. Where indicated, cells were pretreated with different inhibitors for 60 min (25 nM LHVS, 1 μM CA-074, or 25 μM E-64). Proteins were separated by SDS-PAGE on a reducing 12.5% SDS gel, and reactive proteins were visualized by streptavidin blotting ($n=3$). (C) Live human DC were incubated with DCG-0N or PS457 at 25 μM at 4°C or 37°C. Where indicated, DC were matured by addition of LPS 24 h before labeling, and labeling of DC and monocyte-derived cell lysates at 37°C served as controls. The labeled polypeptides were visualized by an antibiotin blot after cell lysis and SDS-PAGE ($n=4$). (D) Intracellular delivery of PS457 in live DC, which were incubated with DCG-0N or PS457 (10 μM each) at 37°C for 10 min (pulse), followed by extensive washing, and a 30-min chase at 37°C. At each time-point, cells were lysed, and the targeted protease polypetides were visualized by a streptavidin blot ($n=3$).

DISCUSSION

MO-DC loaded with antigenic peptide or complex protein represent the basis for several protocols, which aim at therapeutic vaccination in clinical trials. Different strategies are being applied to tailor antigenic material in a way that best exploits the nature of the internalization and processing machinery of MO-DC so that maximum amounts of the antigenic epitope are loaded ultimately on MHC II. Growing evidence indicates that the nature and specificity of the dominant protease(s) that mediate(s) the initial proteolytic attack on antigen after internalization by APC are of critical importance for the generation of a given antigenic epitope [19, 20]. Murine BM-derived macrophages selectively recruit active CatS to internalized material during phagosome maturation, in contrast to murine BM-derived DC [24]. Protease contents and the architecture of endocytic compartments likely differ among various types of APC, DC preparations, and species, so that these results cannot a priori be transferred to human MO-DC. We therefore here aimed at resolving the interaction between endocytic proteases and internalized material in viable human MO-DC. In addition, we evaluated strategies that increase or modulate such delivery of exogenous material to protease-containing compartment(s).

Our results show that human MO-DC efficiently internalize the peptide-like ABP when exposed to the soluble tracer in culture medium, in contrast to internalization via phagocytosis. Exogenous material, as such incorporated, is routed selectively to active CatS, and CatB, CatL, and CatX are only poorly targeted, if at all, by a mechanism that requires activity of the vacuolar H^+-ATPase. This CatS-targeted delivery of exogenous, soluble matter in human DC could be observed as early as 3 min after exposure of DC to the tracer and increased over 20–30 min after internalization. In addition, endosomes of human MO-DC containing the internalized tracer selectively acquired active CatS during maturation. This is not a specific trait for MO-DC but was similarly observed in primary human monocytes. Our data therefore suggest that CatS is a function-

ally dominant, active protease in early endocytic compartments of human monocytes and MO-DC. Fractionation experiments with resolution of endocytic subcompartments revealed a differential distribution of active proteases in human DC, where CatS and CatB polypeptides were present in early endosomes in roughly equal amounts, in contrast to CatX and CatL [22], consistent with our results. We attribute the poor interaction between internalized DCG-0N and active CatB observed here to the only mildly acidic to near-neutral pH present in early endosomes, where CatB is expected to be inactive, in contrast to CatS, which shows a unique stability and activity from acidic up to neutral pH [37]. Thus, the preferential interaction of internalized material with CatS likely represents the combined result of differential distribution of cathepsins in conjunction with the pH gradient along the endocytic route. These results strongly suggest CatS as a functionally dominant endocytic protease likely to initiate antigen breakdown in human MO-DC. However, it cannot be excluded formally that nonpapain proteases, such as active AEP, CatD, or CatE, which cannot be monitored with the probe used here, are reached by an exogenous tracer within a similar time window. However, unlike CatS, none of these proteases has been shown to be active or present in early endosomal compartments, consistent with their low pH optima.

The direct comparison between human MO-DC and murine BM-derived DC resulted in a 1-log lower efficiency of internalization (number of positive cells×mean fluorescence intensity) of identical fluorochrome-coupled latex beads by human MO-DC, and a similar difference was not observed for fluid phase-mediated endocytosis of a soluble protein. Thus, fluid-phase endocytosis appears to be a preferred mode of uptake of exogenous material by MO-DC in vitro. Although it is not entirely clear which route of antigen uptake (endocytosis vs. phagocytosis) is the preferred one for human DC in vivo [1], fluid-phase, mediated endocytosis has been shown to deliver antigen efficiently for T cell activation after vaccination [38, 39] in vivo.

Proteolysis in the endocytic compartment of DC is regulated largely via the maturation state and the activity of the vacuolar ATPase. Although low ATPase activity is found in resting/immature DC with a generally, slightly higher endosomal pH, LPS-mediated stimulation of DC leads to a drop in endocytic pH and more efficient proteolysis [40]. We here demonstrate that changes in the ATPase activity induced by the inhibitor Con B or by LPS-mediated activation indeed modulate the interaction of the internalized tracer with active cathepsins. Inhibition of the ATPase abolished the delivery of the probe to active CatS. This was not a result of inactivation of the protease per se, as demonstrated by labeling of active CatS in cell lysates treated with Con B. Treatment with LPS resulted in an increased labeling of active CatS by the internalized probe at early chase-times, in comparison with nonstimulated controls. This is consistent with the model of a LPS-induced decrease in endocytic pH, which is likely to induce (auto)-catalytic activation of CatS, already in early endocytic compartments, as well as with the redistribution of active CatS to earlier endocytic compartments, as demonstrated for human DC upon LPS stimulation [22]. The intracellular maturation, activation, and degradation of newly synthesized CatS have not yet been addressed. As we here demonstrate by pulse-chase analysis and immunoprecipitation of radiolabeled, newly synthesized protein, CatS is degraded in the endocytic compartment of LPS-stimulated DC within approximately 60 min of entry into the endocytic tract, in contrast to nonstimulated DC, and CatS biosynthesis and the rate of conversion of pro-CatS into its active, mature form are not influenced by DC maturation. Thus LPS-stimulated MO-DC limit the amounts of active CatS by degradation of the newly synthesized enzyme, in contrast to resting DC. This may control the (self-)destructive potential of CatS. However, the overall proteolytic environment of endocytosed antigens does not differ substantially between unstimulated and activated MO-DC.

As active CatS controls Ii maturation and thereby MHC II peptide-loading, a facilitated delivery of exogenous material to CatS-containing compartments might allow improvement of vaccination protocols. Our results demonstrate that targeting of peptide-like, synthetic compounds to active cathepsins in live human DC can be increased substantially by attaching peptide to a protein-size carrier or to a CPP. As internalization of typical, fluid-phase markers such as Dextran or HRP in DC is also mediated, at least in part, by receptor-mediated endocytosis via mannose receptor-binding [35, 36], we suggest that the improved internalization of the DCG-0N-streptavidin complex may also rely on this additional mode of uptake.

CPP-enhanced endocytic uptake was clearly the most efficient way of internalization into MO-DC. Despite their broad acceptance as molecular carriers, the mechanism of internalization of polycationic peptides is not well understood, and active, endocytosis-mediated as well as passive transition of the membrane is still under debate [28]. As PS457 labeled active cathepsins in intact cells also at 4°C, we strongly argue that CPP can enter the DC efficiently, independently from energy-dependent mechanisms such as endocytosis. However, endocytosis clearly improves the uptake of PS457 into cathepsin-containing compartments, as shown by appropriate changes at 37°C and after LPS-induced down-regulation of macropinocytosis, respectively. Although the selective transport to CatS is preserved when macropinocytosis is facilitated by conjugation of the probe to a protein carrier, this type of selectivity is lost when internalization is achieved by CPP. We suggest that soluble peptide or peptide attached to a protein carrier only reaches a subpopulation of endocytic compartments enriched in CatS activity and separated from conventional, late endosomes/lysosomes by membrane barriers. We envision that CPP may transit these separating membranes after internalization by MO-DC and hence, gain access to the entire spectrum of endocytic protease activity.

Conjugation of the immunogenic peptide to a CPP carrier prior to vaccination resulted in a vaccination success and a CD4-T cell-dependent tumor regression as a result of sustained antigen presentation in a murine model for peptide-based cancer immunotherapy, and the same peptide without a CPP carrier proved ineffective [29]. As demonstrated here, such conjugation of peptide to CPP greatly increases transport to CatS-containing, endocytic compartments as well as to endocytic proteases in general. Both aspects might lead to improved antigen processing and MHC II-peptide loading and hence, explain the sustained antigen presentation observed when an-

tigen was delivered via CPP in vivo. In this sense, conjugation of antigen to CPP might serve as a universal strategy to shuttle antigenic peptide to the MHC II processing machinery. It should be noted, however, that facilitated delivery of antigenic protein to endocytic proteases (or to a broader selection of proteases) might also bear the potential to impair antigen presentation as a result of destructive processing. This likely depends on the nature and the processing pathway of the antigen used [18–20].

As we here identify CatS as a major protease reached by such constructs, conjugation of antigen to CPP via a CatS-sensitive peptide bond might be a worthwhile strategy to selectively release antigenic material in the appropriate compartment. In addition, conjugation of antigenic peptide to CPP may allow achievement of sufficient internalization of antigen and its delivery to proteases, even in LPS-activated DC, which are highly immunogenic but poorly endocytotic. Clearly, these possible applications of CPP warrant further systematic investigation with respect to the T cell response elicited in vitro and in vivo.

ACKNOWLEDGMENTS

This work was supported by grants from the Deutsche Forschungsgemeinschaft (DR378.2-3, SFB 685), the Federal Ministry of Education and Research (Fö.01KS9602), the Interdisciplinary Centre of Clinical Research Tübingen (IZKF), and the Marie Curie Research Training Network "Drugs for Therapy."

REFERENCES

1. Trombetta, E. S., Mellman, I. (2005) Cell biology of antigen processing in vitro and in vivo. *Annu. Rev. Immunol.* **23,** 975–1028.
2. Mellman, I., Steinman, R. M. (2001) Dendritic cells: specialized and regulated antigen processing machines. *Cell* **106,** 255–258.
3. Steinman, R. M., Pack, M., Inaba, K. (1997) Dendritic cell development and maturation. *Adv. Exp. Med. Biol.* **417,** 1–6.
4. Rossi, M., Young, J. W. (2005) Human dendritic cells: potent antigen-presenting cells at the crossroads of innate and adaptive immunity. *J. Immunol.* **175,** 1373–1381.
5. Fiebiger, E., Meraner, P., Weber, E., Fang, I. F., Stingl, G., Ploegh, H., Maurer, D. (2001) Cytokines regulate proteolysis in major histocompatibility complex class II-dependent antigen presentation by dendritic cells. *J. Exp. Med.* **193,** 881–892.
6. Burster, T., Beck, A., Tolosa, E., Schnorrer, P., Weissert, R., Reich, M., Kraus, M., Kalbacher, H., Haring, H. U., Weber, E., Overkleeft, H., Driessen, C. (2005) Differential processing of autoantigens in lysosomes from human monocyte-derived and peripheral blood dendritic cells. *J. Immunol.* **175,** 5940–5949.
7. Chain, B. M., Free, P., Medd, P., Swetman, C., Tabor, A. B., Terrazzini, N. (2005) The expression and function of cathepsin E in dendritic cells. *J. Immunol.* **174,** 1791–1800.
8. Shi, G. P., Bryant, R. A., Riese, R., Verhelst, S., Driessen, C., Li, Z., Bromme, D., Ploegh, H. L., Chapman, H. A. (2000) Role for cathepsin F in invariant chain processing and major histocompatibility complex class II peptide loading by macrophages. *J. Exp. Med.* **191,** 1177–1186.
9. Driessen, C., Bryant, R. A., Lennon-Dumenil, A. M., Villadangos, J. A., Bryant, P. W., Shi, G. P., Chapman, H. A., Ploegh, H. L. (1999) Cathepsin S controls the trafficking and maturation of MHC class II molecules in dendritic cells. *J. Cell Biol.* **147,** 775–790.
10. Driessen, C., Lennon-Dumenil, A. M., Ploegh, H. L. (2001) Individual cathepsins degrade immune complexes internalized by antigen-presenting cells via Fcγ receptors. *Eur. J. Immunol.* **31,** 1592–1601.
11. Riese, R. J., Wolf, P. R., Bromme, D., Natkin, L. R., Villadangos, J. A., Ploegh, H. L., Chapman, H. A. (1996) Essential role for cathepsin S in the MHC class II-associated invariant chain proecessing and peptide loading. *Immunity* **4,** 357–366.
12. Nakagawa, T., Roth, W., Wong, P., Nelson, A., Farr, A., Deussing, J., Villadangos, J. A., Ploegh, H., Peters, C., Rudensky, A. Y. (1998) Cathepsin L: critical role in Ii degradation and CD4 T cell selection in the thymus. *Science* **280,** 450–453.
13. Riese, R. J., Mitchell, R. N., Villadangos, J. A., Shi, G. P., Palmer, J. T., Karp, E. R., De Sanctis, G. T., Ploegh, H. L., Chapman, H. A. (1998) Cathepsin S activity regulates antigen presentation and immunity. *J. Clin. Invest.* **101,** 2351–2363.
14. Shi, G. P., Villadangos, J. A., Dranoff, G., Small, C., Gu, L., Haley, K. J., Riese, R., Ploegh, H. L., Chapman, H. A. (1999) Cathepsin S required for normal MHC class II peptide loading and germinal center development. *Immunity* **10,** 197–206.
15. Nakagawa, T. Y., Brissette, W. H., Lira, P. D., Griffiths, R. J., Petrushova, N., Stock, J., McNeish, J. D., Eastman, S. E., Howard, E. D., Clarke, S. R., Rosloniec, E. F., Elliott, E. A., Rudensky, A. Y. (1999) Impaired invariant chain degradation and antigen presentation and diminished collagen-induced arthritis in cathepsin S null mice. *Immunity* **10,** 207–217.
16. Honey, K., Nakagawa, T., Peters, C., Rudensky, A. (2002) Cathepsin L regulates CD4+ T cell selection independently of its effect on invariant chain: a role in the generation of positively selecting peptide ligands. *J. Exp. Med.* **195,** 1349–1358.
17. Pierre, P., Mellman, I. (1998) Developmental regulation of invariant chain proteolysis controls MHC class II trafficking in mouse dendritic cells. *Cell* **93,** 1135–1145.
18. Manoury, B., Hewitt, E. W., Morrice, N., Dando, P. M., Barrett, A. J., Watts, C. (1998) An asparaginyl endopeptidase processes a microbial antigen for class II MHC presentation. *Nature* **396,** 695–699.
19. Manoury, B., Mazzeo, D., Fugger, L., Viner, N., Ponsford, M., Streeter, H., Mazza, G., Wraith, D. C., Watts, C. (2002) Destructive processing by asparagine endopeptidase limits presentation of a dominant T cell epitope in MBP. *Nat. Immunol.* **3,** 169–174.
20. Watts, C., Moss, C. X., Mazzeo, D., West, M. A., Matthews, S. P., Li, D. N., Manoury, B. (2003) Creation versus destruction of T cell epitopes in the class II MHC pathway. *Ann. N. Y. Acad. Sci.* **987,** 9–14.
21. Lautwein, A., Kraus, M., Reich, M., Burster, T., Brandenburg, J., Overkleeft, H. S., Schwarz, G., Kammer, W., Weber, E., Kalbacher, H., Nordheim, A., Driessen, C. (2004) Human B lymphoblastoid cells contain distinct patterns of cathepsin activity in endocytic compartments and regulate MHC class II transport in a cathepsin S-independent manner. *J. Leukoc. Biol.* **75,** 844–855.
22. Lautwein, A., Burster, T., Lennon-Dumenil, A. M., Overkleeft, H. S., Weber, E., Kalbacher, H., Driessen, C. (2002) Inflammatory stimuli recruit cathepsin activity to late endosomal compartments in human dendritic cells. *Eur. J. Immunol.* **32,** 3348–3357.
23. Greiner, A., Lautwein, A., Overkleeft, H. S., Weber, E., Driessen, C. (2003) Activity and subcellular distribution of cathepsins in primary human monocytes. *J. Leukoc. Biol.* **73,** 235–242.
24. Lennon-Dumenil, A. M., Bakker, A. H., Maehr, R., Fiebiger, E., Overkleeft, H. S., Rosemblatt, M., Ploegh, H. L., Lagaudriere-Gesbert, C. (2002) Analysis of protease activity in live antigen-presenting cells shows regulation of the phagosomal proteolytic contents during dendritic cell activation. *J. Exp. Med.* **196,** 529–540.
25. Greenbaum, D., Medzihradszky, K. F., Burlingame, A., Bogyo, M. (2000) Epoxide electrophiles as activity-dependent cysteine protease profiling and discovery tools. *Chem. Biol.* **7,** 569–581.
26. Tolosa, E., Li, W., Yasuda, Y., Wienhold, W., Denzin, L. K., Lautwein, A., Driessen, C., Schnorrer, P., Weber, E., Stevanovic, S., Kurek, R., Melms, A., Bromme, D. (2003) Cathepsin V is involved in the degradation of invariant chain in human thymus and is overexpressed in myasthenia gravis. *J. Clin. Invest.* **112,** 517–526.
27. Burster, T., Beck, A., Tolosa, E., Marin-Esteban, V., Rotzschke, O., Falk, K., Lautwein, A., Reich, M., Brandenburg, J., Schwarz, G., Wiendl, H., Melms, A., Lehmann, R., Stevanovic, S., Kalbacher, H., Driessen, C. (2004) Cathepsin G, and not the asparagine-specific endoprotease, controls the processing of myelin basic protein in lysosomes from human B lymphocytes. *J. Immunol.* **172,** 5495–5503.
28. Fischer, R., Fotin-Mleczek, M., Hufnagel, H., Brock, R. (2005) Break on through to the other side—biophysics and cell biology shed light on cell-penetrating peptides. *ChemBioChem* **6,** 2126–2142.
29. Wang, R. F., Wang, H. Y. (2002) Enhancement of antitumor immunity by prolonging antigen presentation on dendritic cells. *Nat. Biotechnol.* **20,** 149–154.
30. Lutz, M. B., Kukutsch, N., Ogilvie, A. L., Rossner, S., Koch, F., Romani, N., Schuler, G. (1999) An advanced culture method for generating large

quantities of highly pure dendritic cells from mouse bone marrow. *J. Immunol. Methods* **223,** 77–92.
31. Van Swieten, P. F., Maehr, R., Van Den Nieuwendijk, A. M., Kessler, B. M., Reich, M., Wong, C. S., Kalbacher, H., Leeuwenburgh, M. A., Driessen, C., Van Der Marel, G. A., Ploegh, H. L., Overkleeft, H. S. (2004) Development of an isotope-coded activity-based probe for the quantitative profiling of cysteine proteases. *Bioorg. Med. Chem. Lett.* **14,** 3131–3134.
32. Palmer, J. T., Rasnick, D., Klaus, J. L., Bromme, D. (1995) Vinyl sulfones as mechanism-based cysteine protease inhibitors. *J. Med. Chem.* **38,** 3193–3196.
33. Wiendl, H., Lautwein, A., Mitsdorffer, M., Krause, S., Erfurth, S., Wienhold, W., Morgalla, M., Weber, E., Overkleeft, H. S., Lochmuller, H., Melms, A., Tolosa, E., Driessen, C. (2003) Antigen processing and presentation in human muscle: cathepsin S is critical for MHC class II expression and upregulated in inflammatory myopathies. *J. Neuroimmunol.* **138,** 132–143.
34. Benaroch, P., Yilla, M., Raposo, G., Ito, K., Miwa, K., Geuze, H. J., Ploegh, H. L. (1995) How MHC class II molecules reach the endocytic pathway. *EMBO J.* **14,** 37–49.
35. Sallusto, F., Cella, M., Danieli, C., Lanzavecchia, A. (1995) Dendritic cells use macropinocytosis and the mannose receptor to concentrate macromolecules in the major histocompatibility complex class II compartment: downregulation by cytokines and bacterial products. *J. Exp. Med.* **182,** 389–400.
36. Garrett, W. S., Chen, L. M., Kroschewski, R., Ebersold, M., Turley, S., Trombetta, S., Galan, J. E., Mellman, I. (2000) Developmental control of endocytosis in dendritic cells by Cdc42. *Cell* **102,** 325–334.
37. Chapman, H. A., Riese, R. J., Shi, G. P. (1997) Emerging roles for cysteine proteases in human biology. *Annu. Rev. Physiol.* **59,** 63–88.
38. Delamarre, L., Pack, M., Chang, H., Mellman, I., Trombetta, E. S. (2005) Differential lysosomal proteolysis in antigen-presenting cells determines antigen fate. *Science* **307,** 1630–1634.
39. Zhong, G., Reis e Sousa, C., Germain, R. N. (1997) Antigen-unspecific B cells and lymphoid dendritic cells both show extensive surface expression of processed antigen-major histocompatibility complex class II complexes after soluble protein exposure in vivo or in vitro. *J. Exp. Med.* **186,** 673–682.
40. Trombetta, E. S., Ebersold, M., Garrett, W., Pypaert, M., Mellman, I. (2003) Activation of lysosomal function during dendritic cell maturation. *Science* **299,** 1400–1403.